Comprehensive Study of the Influence of the Bonding Temperature and Contact Pressure Regimes during Diffusion Bonding on the Deformation and Mechanical Properties of AISI 304

Thomas Gietzelt,* Mario Walter, Volker Toth, Florian Messerschmidt, and Melina Blem

Process parameters for diffusion bonding are temperature, dwell time, and contact pressure. Temperature and contact pressure have opposite effects on deformation. The effect of temperature on deformation was investigated in steps of 20 K from 1015 to 1135 °C. Contact pressure and dwell time were 16 MPa and 4 h, respectively. The deformation increase steadily with temperature. Yield strength and tensile strength decrease slightly with temperature, which is attributed to grain growth. The elongation-at-fracture values are 100–105%. For 925 to 995 °C, values for elongation at fracture decrease. It was investigated if comparable mechanical properties can be obtained at a temperature of 850 °C only. Experiments with higher constant contact pressures were supplemented by tests with superimposed short load peaks. Similar and higher values for the yield strength were achieved. A correlation of yield strength, tensile strengths and elongation-at-fracture values with contact pressure and contact pressure regime was found. The values for elongation at fracture are significantly lower than those for higher temperatures. This even applies to parameter sets at different temperatures, leading to almost identical deformations. Reduced elongation-at-fracture values at 850 °C are attributed to microscopically small defects in the bonding plane and to notch effects.

1. Introduction

Diffusion bonding is an elaborate technique to create full cross-sectional bonding of complex structured components. It is performed at 80–90% of a material's melting range calculated in kelvin and is always accompanied by deformation. Surprisingly, the role of deformation and its relation to the mechanical properties of diffusion-bonded joints is rarely addressed in the literature.

Contributions to deformation can be divided into a fraction of the microscopic leveling of the surface roughness and the plastic flow of the material as a function of the bonding temperature, contact pressure, and dwell time. It is concentrated in mechanically microstructured areas with reduced contact surfaces and causes pressure loss and a decrease in the throughput of media in microchannels.

For multilayered devices, depending on the design, the bonding cross section, and, therefore, the contact pressure, may vary from layer to layer. The question of force transmission, i.e., force distribution over several layers to achieve a reproducible joining result over the whole part, was investigated.[1]

Depending on the size of the cross-sectional area to be joined, the number of layers, and the thickness tolerances of the sheet metal production, additional technical contributions to the deformation are possible to establish the atomic contact between all surfaces and to obtain a uniform contact pressure. This contribution to deformation is design and component dependent. It may cause different deformations despite constant joining parameters for identical components.

After approaching the mating surfaces, the contact area is increased at microscopic level with time by diffusion along the grain boundaries and interfaces, since the atomic density here is lower and, therefore, the coefficient of diffusion is some orders of magnitude higher than in the metallic lattice itself.[2] The dwell time, however, is responsible for closing remaining pores between deformed asperities by volume diffusion at a much lower coefficient of diffusion.[3]

Ideally, after diffusion bonding according to diffusion bonding theory, the mechanical properties of a part should be identical to those of a material subjected to an identical heat treatment. Otherwise, there are imperfections in the bonding plane, or brittle phases have been formed. Different coefficients of diffusion

Dr. T. Gietzelt, V. Toth, F. Messerschmidt
Institute for Micro Process Engineering
KIT
Post Box 3640, 76 021 Karlsruhe, Germany
E-mail: thomas.gietzelt@kit.edu

Dr. M. Walter, M. Blem
Institute for Applied Materials
KIT
Post Box 3640, 76 021 Karlsruhe, Germany

**ADVANCED
SCIENCE NEWS**
www.advancedsciencenews.com

**ADVANCED
ENGINEERING
MATERIALS**
www.aem-journal.com

and a higher affinity of alloying elements may be reasons for this, e.g., when bonding different materials, or precipitates at grain boundaries for complex alloys are formed.[4–8]

In the literature, only little attention is paid to the impact on deformation of leveling multiple surface roughnesses of multi-layered devices.[3] This may be because that diffusion-bonded parts in most cases consist of a few layers only. It was shown by the authors that the impact of the number of layers on deformation cannot be neglected.[9,10]

However, the main impact on deformation is the materials flow rate depending on the bonding temperature and contact pressure. Since the concentration of vacancies in metallic lattice follows an exponential function, it approximately doubles when increasing the bonding temperature by 20 K at about 80% of the melting range, causing a huge impact on deformation. Therefore, temperature measurement and homogeneity of the temperature are of great interest to the diffusion bonding process.

During diffusion bonding, due to high temperatures and long dwell times, the dislocation density is drastically reduced and grain growth occurs. The grain growth depends strongly on the absolute bonding temperature and exhibits no linear behavior. For example, for titanium, it was shown that excessive grain growth starts at 900 °C.[11] According to the *Hall–Petch* relation, an increasing grain size will decrease strength since grain boundaries are obstacles limiting dislocation movement across the metallic lattice.[12] If materials exhibit no polymorphy, their microstructure is much coarser after diffusion bonding. Therefore, lower strength values can be expected for samples diffusion bonded at higher temperatures as shown in this article.[13]

If cold work-hardened materials are used, recrystallization may facilitate grain growth across the bonding planes and limit grain growth, as polymorphy does in the case of mild steel.[14–17] During diffusion bonding in high vacuum, only limited cooling rates can be realized. For nickel-base alloys, however, this facilitates the formation of precipitations at grain boundaries, which is bad in terms of corrosion resistance.[18,19]

Many publications reporting mechanical properties of diffusion bonds lack in information on deformation[20] or data for the statistical validation of given values.[14,15,21,22]

Reduced elongation-at-fracture values and varying tensile strengths indicate that the bonding parameters influence the mechanical properties of the bonds.[20,23]

Since bonding temperature and contact pressure have opposite effects, similar strength values can be achieved under different conditions.

For corrosion-resistant alloys, the formation, thickness, and composition of passivation layers strongly influence the ability of diffusion bonding. At low bonding temperatures and applying high contact pressures, asperities can help to destroy the integrity of passivation layers, promoting diffusion. In addition, grain growth is reduced at lower temperatures. The coefficient of diffusion, however, may drop several orders of magnitude, impeding grain growth across the bond line and filling the remaining pores.

Achieving adequate deformation during diffusion bonding for opposing values of bonding temperature and contact pressure does not guarantee reasonable elongation-to-fracture values, as shown here.

In consequence, diffusion bonding parameters must not only be optimized in terms of mechanical properties of the bond but also regarding the alloys' composition.

In this article, diffusion bonding experiments on austenitic stainless steel 304 at a low joining temperature of 850 °C and varying contact pressure were performed. For reasons of comparison, an additional experiment was performed at 800 °C, too.

Practically, it is difficult to adjust a contact pressure so that a certain percentage of deformation is obtained. Therefore, additional experiments were conducted combining a constant contact pressure with several short-term peak contact pressures. By superimposing of peak loads, where a much higher creep rate occurs, the bonding area at microscopic scale is increased, whereas the absolute amount of deformation is limited due to the short duration. In consequence, a higher creep rate due to deviation of temperature and the design of the part will not cause improper distortions either and will help to control the overall deformation.

The deformation and mechanical properties of bonding experiments at 850 °C were compared to those obtained from experiments at a constant contact pressure of 16 MPa. For this, experiments within a temperature range of $T = 925$–1135 °C were performed.

2. Materials and Design of Experiments

As material, round stock 20 and 40 mm in diameter of austenitic stainless steel 1.4301 (AISI 304) was used. The delivery condition was solution annealed. From this, cylinders were turned 20 and 40 mm in height, respectively, at a tolerance of ±0.05 mm. For diffusion bonding experiments, two cylinders were stacked, so the aspect ratio was two for both diameters (**Figure 1**). The dwell time was set to $t = 4$ h. Since the maximum force of the furnace used was 20 kN, a contact pressure of 15.9 MPa results for the $d = 40$ mm samples. For simplifying reasons, this contact pressure is rounded up to 16 MPa in this publication. Therefore, the samples of both diameters can be diffusion bonded in one furnace.
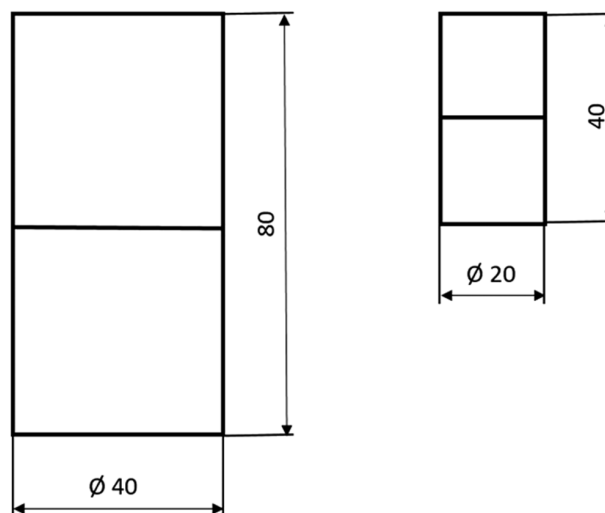

Figure 1. Scheme of diffusion bonding samples $d = 40$ and 20 mm.

**ADVANCED
SCIENCE NEWS**
www.advancedsciencenews.com

**ADVANCED
ENGINEERING
MATERIALS**
www.aem-journal.com

The bonding temperature was monitored and controlled using a thermocouple type S (Pt/PtRh10) consisting of two wires 0.3 mm in diameter and laser-welded at the tip. The wires were insulated by segments of alumina ferrules 4 mm in diameter with two internal holes. They were mounted on the sample by means of a small block made of molybdenum with a hole for it.

Starting at 1075 °C, the bonding temperature was varied in steps of 20 K within a range where the deformation for the samples 40 mm in diameter was below 20% but high enough to limit measuring errors.

For samples bonded at $T = 850$ °C, a dwell time of $t = 4$ h, contact pressures of more than 16 MPa, and a furnace with 200 kN maximum force were used. In a first step, different levels of contact pressure were investigated for comparison with deformations obtained at much higher bonding temperatures in the first set of experiments. After determining the contact pressure at 850 °C where the material starts to deform, various experiments with peak loads were performed.

3. Experiments and Results

3.1. Characterization of Surface Roughness

The finely turned surfaces of the cylindrical samples were characterized by means of a *Sensofar S neox* by Sensofar Metrology, Terrassa, Spain, with respect to roughness. A combination of focus variation and confocal microscopy mode was used. In the center, an area of about 1.8×1.3 mm was evaluated (**Figure 2**A,B). The line profile in Figure 2B shows roughness values of $R_a = 4.6$ µm and $R_t = 31.8$ µm. Areas with greater roughness are visible in the center of the sample, which is formed during cutting of tough austenitic stainless steel due to the formation of built-up edges at the lathe tool with decreasing cutting speed in the center.

A series of 29 images with 20% overlap each were stitched, covering the full sample diameter of 40 mm. To the whole sample, diameter of 40 mm, roughness values of $R_a = 4.0$ µm, and $R_t = 52.2$ µm apply (Figure 2C).

3.2. Setup of Diffusion Bonding Experiments

For all diffusion bonding experiments, additional baffle plates made of TZM were used to protect the pressure dies from getting damaged. The baffle plates were coated with alumina suspension to prevent sticking at the samples. After placing the samples in the furnace, it was evacuated to a vacuum better than $1 * E-04$ mbar. When reaching this threshold, the temperature was ramped up at a rate of 10 K min^{-1}. The load was applied after reaching the set point of temperature within 5 min. After diffusion bonding, the temperature was decreased at a rate of 10 K min^{-1}. Depending on the size and thermal mass of the furnace, the natural cooling rate was less than 10 K min^{-1}, starting at about 600 °C.

For each set of parameters, one diffusion bonding experiment was performed.

3.3. $\Delta T = 20$ K Experiments for Samples $d = 20$ and $d = 40$ mm, AR = 2 at $p = 16$ MPa

For each set of parameters, one bonding experiment was performed. For round stock 40 mm in diameter and 40 mm $\pm$ 0.05 mm in height, as well as 20 mm in diameter and 20 mm $\pm$ 0.05 mm in height, two pieces were stacked inside the furnace. The calculation of the percentage deformation is based on the initial height of 80 and 40 mm, respectively. The samples were diffusion bonded using a variation of temperature in steps of 20 K, around $T = 1075$ °C, for $t = 4$ h and $p = 16$ MPa. For the maximum temperature, a percentaged deformation of 20% was set as threshold for practical reasons.
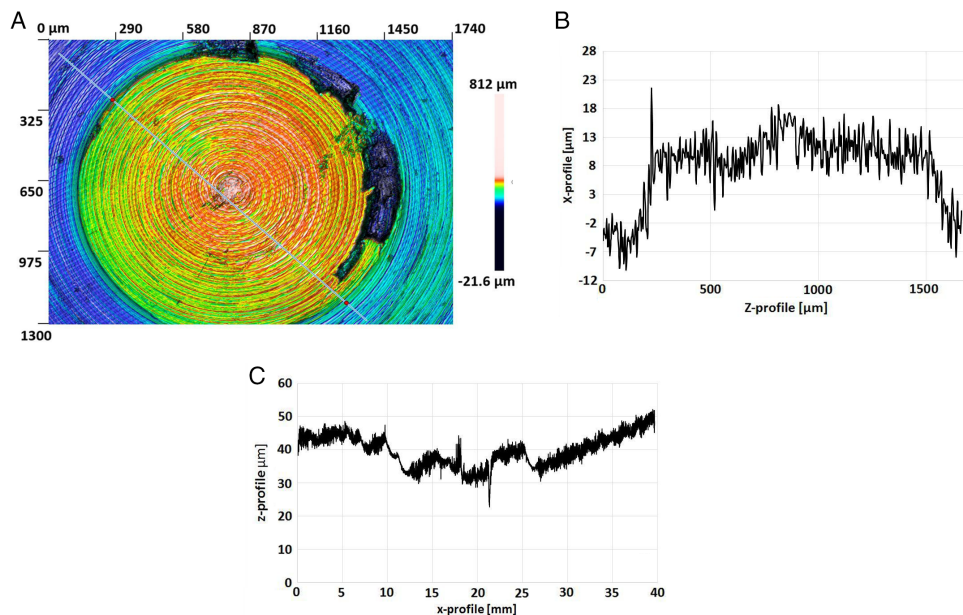

Figure 2. Characterization of surface roughness. A) Overview center. B) Roughness profile at the center. C) Roughness profile over the whole sample diameter.

**ADVANCED
SCIENCE NEWS**
www.advancedsciencenews.com

**ADVANCED
ENGINEERING
MATERIALS**
www.aem-journal.com

All diffusion bonding experiments were performed in a furnace with a maximum bonding force of 20 kN. From this, to the samples 40 mm in diameter, a contact pressure of 16 MPa is applied. For samples 20 mm in diameter, however, a load of 5 kN was used to obtain identical contact pressures. The results of deformation are summarized in **Table 1**. Comparing the deformation for samples 40 mm in diameter obtained for $T = 1015\,°C$ to the standard bonding temperature of $T = 1075\,°C$, a temperature rise of 60 K led to an increase in deformation of 250%. This underlines the nonlinear impact of temperature on deformation. Raising the temperature for another 60 K to $1135\,°C$, the deformation doubles compared to $T = 1075\,°C$ and reaches nearly 20%. From other experiments, deformations were added for lower temperatures. For a bonding temperature of $T = 925\,°C$ only, the deformation starts vanishing and is about one fifteenth of that at $T = 1075\,°C$. For such low deformation, no good mechanical properties were expected.

Figure 3 shows the deformation for both sample diameters versus temperature. The deformation increased steadily for all samples, raising the bonding temperature in steps of 20 K. For some experiments, however, the increase in deformation was not increased steadily (bold values in Table 1). For $d = 40\,mm$, this was for $T = 995$, 1015, and $1115\,°C$, for $d = 20\,mm$ for $T = 1095$ and $1115\,°C$.

At a bonding temperature of $850\,°C$, no deformation can be detected.

From Table 1, it can be seen that there are only slight deviations in deformation for samples 20 and 40 mm in diameter. This is in contradiction to the findings in the study by Gietzelt et al.[9] It is attributed to small cross sections in combination with the high aspect ratio of $AR = 2$. Thus, the friction at the pressure dies does not rule deformation behavior.

Figure 4 shows the bonding cross section for a contact pressure of $p = 16\,MPa$ and a dwell time of $t = 4\,h$ for $T = 850\,°C$, the standard bonding temperature of $T = 1075\,°C$, and $T = 1135\,°C$. For $T = 85\,°C$, a poor bonding quality can be seen, displaying a line of pores due to zero deformation. For 1075 and $1135\,°C$,
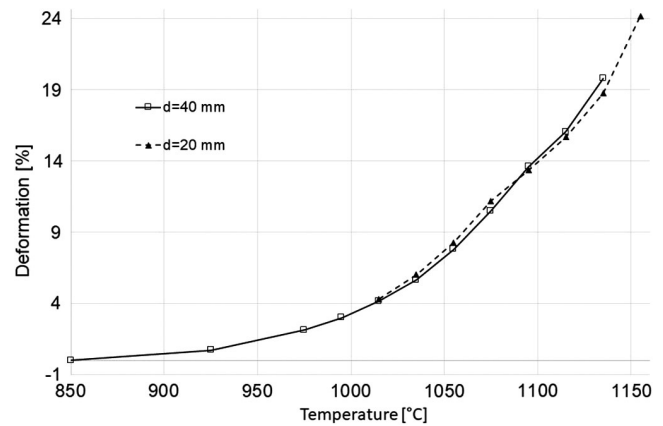

Figure 3. Temperature-dependent deformation for $t = 4\,h$, $p = 16\,MPa$, T-steps of 20 K.

however, the original bonding cross section cannot be detected anymore. It is marked by arrows indicating the bonding cross section at the outlines of the samples. For $T = 1135\,°C$, the grain sizes are larger than for $T = 1075\,°C$.

Since zero deformation was detected at $T = 850\,°C$, $p = 16\,MPa$, and $t = 4\,h$, and parameters are far away from our experience, the sample was fixed in a bench vise and struck using a sledge. However, it could not be detached and, therefore, samples for tensile tests were manufactured.

3.4. Diffusion Bonding Tests at $T = 850\,°C$ for Constant and Superimposed Peak Contact Pressures

Diffusion bonding experiments at $T = 850\,°C$ were performed in furnace I (max. load 20 kN) for 16 MPa and in furnace II (max. load 200 kN) for higher contact pressures at samples 40 mm in diameter. These parameters were chosen due to the study by Elßner et al.,[24] where good bonding results can be achieved

Table 1. Impact of temperature on the deformation for samples $d = 40$ and $d = 20\,mm$ $(AR = 2)$ for $t = 4\,h$, $p = 16\,MPa$. Bold values: smaller Δ deformation than at the previous temperature.

Temperature [°C]	$d = 40\,mm$			$d = 20\,mm$		
	Height after diffusion bonding [mm]	Deformation [%]	Δ Deformation to previous temperature [%]	Height after diffusion bonding [mm]	Deformation [%]	Δ Deformation to previous temperature [%]
850	80	0.00		40	0.00	
925	79.43	0.71	0.71			
975	78.29	2.14	1.43			
995	77.6	3.00	**0.86**			
1015	76.67	4.16	**1.16**	38.28	4.30	4.30
1035	75.49	5.64	1.48	37.59	6.03	1.73
1055	73.75	7.81	2.17	36.69	8.28	2.25
1075	71.6	10.50	2.69	35.52	11.20	2.92
1095	69.13	13.59	3.09	34.66	13.35	**2.15**
1115	67.15	16.06	**2.47**	33.73	15.68	**2.33**
1135	64.17	19.79	3.73	32.5	18.75	3.07
1155				30.33	24.18	5.43

**ADVANCED
SCIENCE NEWS**
www.advancedsciencenews.com

**ADVANCED
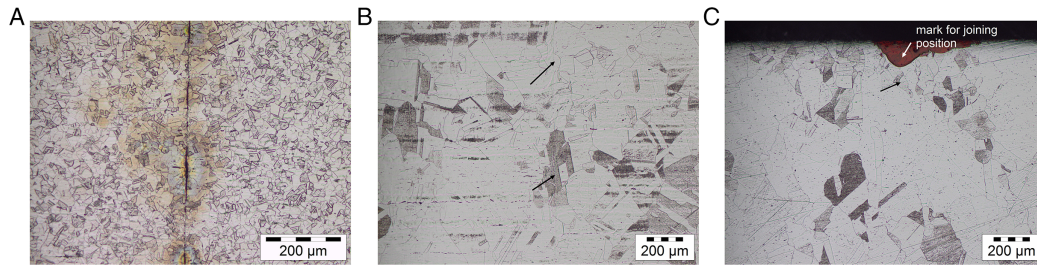ENGINEERING
MATERIALS**
www.aem-journal.com

Figure 4. Microstructure after $t = 4$ h, $p = 16$ MPa of. A) $T = 850\,°C$. B) $T = 1075\,°C$. C) $T = 1135\,°C$.

Table 2. Deformations obtained for samples $d = 40$ mm for constant and peak contact pressures at $T = 850\,°C$, $t = 4$ h.

	p [MPa]	t [h]	Height after diff. bond. [mm]	Deformation [%]	Flow rate [% h^{-1}]
Sample 1	16	4	80	0	
Sample 2	64	4	73.03	8.38	2.095
Sample 3	16	**16**	80	0	
Sample 4	32	4	79.75	0.31	0.0775
Sample 5	$32 + 4 \times 64/1'$	4	79.25	0.94	
Sample 6	$32 + 4 \times 64/5'$	4	78.58	1.76	
Sample 7	$32 + 4 \times 96/1'$	4	76.56	4.3	

by removing the passivation layers on austenitic stainless steel inside a glove box with inert atmosphere prior to bonding.

In **Table 2**, different contact pressure regimes for diffusion bonding experiments performed at $T = 850\,°C$ are summarized. Since this joining temperature is 225 K lower than the joining temperature of $T = 1075\,°C$, which is standard for austenitic stainless steels at the Institute for Micro Process Engineering, the contact pressure to achieve a reasonable deformation is much higher. It was found that for a contact pressure of $p = 16$ MPa, no deformation occurred at 850 °C. Raising the dwell time by four-fold to $t = 16$ h resulted in no deformation, too.

At a contact pressure of $p = 32$ MPa (40 kN), only a slight deformation of 0.31% was obtained. This means that a constant contact pressure of $p = 32$ MPa at a dwell time of $t = 4$ h does not cause serious deformation for this geometry. However, for complex geometries and mechanical microstructures, higher deformation may occur.

For a contact pressure of $p = 64$ MPa (80 kN), the deformation rose to 8.38%, illustrating the nonlinear impact of contact pressure on deformation. This deformation is too high for parts consisting of a few layers only. From this observation, it was concluded that it is almost impossible to control the deformation for arbitrary designs while applying a constant contact pressure. However, short phases at higher contact pressure, at which a higher flow rate of the material applies, should be helpful bringing surfaces into intimate contact and controlling the deformation.

Therefore, for further experiments, a constant level of $x = 32$ MPa of contact pressure was superimposed by short peak loads (see **Figure 5**). The dwell time was fixed at $t = 4$ h. The contact pressure was raised within 1 min to the peak contact
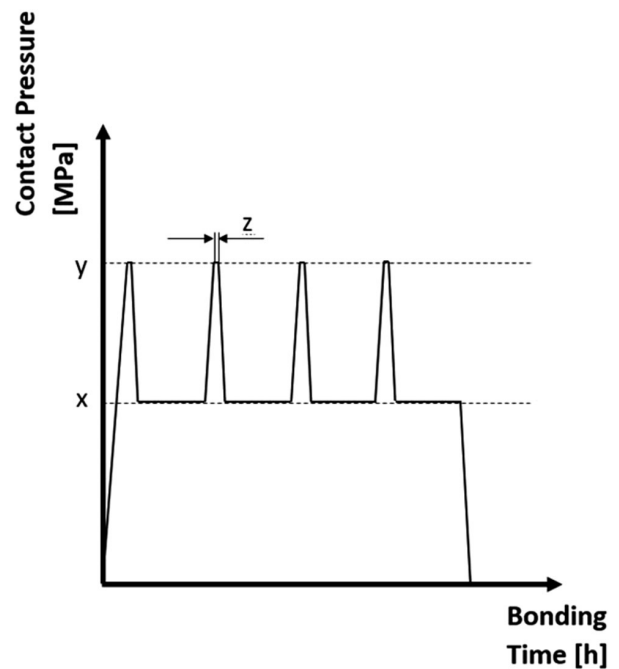

Figure 5. Diffusion bonding process with superimposed peak contact pressures.

pressure, kept constant for a certain time (z), and afterward decreased again within 1 min back to $p = 32$ MPa. Four peak contact pressures, one per hour, were applied. By the initial peak contact pressure, asperities were deformed, increasing the contact area at a microscopic scale. Peak contact pressures of $y = 64$ MPa were applied for $z = 1$ (sample 5) and $z = 5$ min (sample 6), respectively, leading to reasonable deformation values. Also, for a peak contact pressure of $y = 96$ MPa and a dwell time of $z = 1$ min (sample 7), a reasonable deformation of 4.3% was obtained. It has to be pointed out, however, that this deformation is only about 50% of the deformation obtained for a constant contact pressure of $p = 64$ MPa and a dwell time of $t = 4$ h. However, a deformation of 4.3% is close to 4.13% obtained for $T = 1015\,°C$ and $p = 16$ MPa. Therefore, mechanical properties, namely, tensile strength and elongation at fracture, of samples with comparable deformations but different bonding temperatures, were of great interest.

Similar experiments with superimposed peak contact pressure were performed,[25,26] however, at higher frequencies and shorter
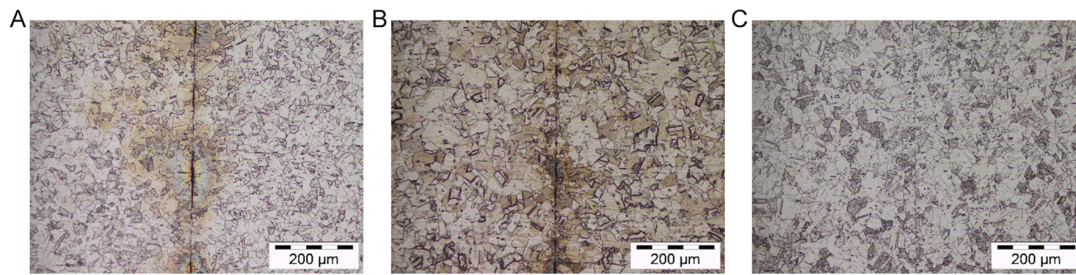
**ADVANCED
SCIENCE NEWS**
www.advancedsciencenews.com

**ADVANCED
ENGINEERING
MATERIALS**
www.aem-journal.com

Figure 6. Bond quality at $T = 850\,°C$, $t = 4\,h$ depending on constant contact pressure: A) $p = 16\,MPa$. B) $p = 32\,MPa$. C) $p = 64\,MPa$.

dwell times in between. However, the authors of this publication are convinced that after a peak load with intentional plastic deformation, a longer dwell time is required to fill pores by volume diffusion.

Figure 6 shows the bonding quality at $T = 850\,°C$ for different contact pressures. In Table 2, flow rates for contact pressures of $p = 32$ and $64\,MPa$, respectively, are calculated. Using these values for calculating expected deformations for experiments using short peak loads (sample 5 or 6) leads to significantly lower values. Obviously, non-negligible deformations occur during loading and unloading periods. Specific deformations for short increased contact pressures are higher than those for constant contact pressures and long dwell times.

3.5. Diffusion Bonding Tests for $t = 4\,h$ at $T = 995, 975,$ and $925\,°C$ at $p = 16\,MPa$ and $T = 800\,°C$, $p = 64\,MPa$

During the tensile tests, it turned out that for all samples for the temperature range of $T = 1015$ to $1135\,°C$, the elongations at fracture were constant, ranging from 100% to 105%.

For all diffusion experiments performed at $T = 850\,°C$, however, regardless of the contact pressure or contact pressure regime, the elongation-at-fracture values were considerably reduced. In fact, this was an expected finding since the coefficient of diffusion is reduced by several orders of magnitudes at $T = 850\,°C$. However, as to be discussed later, superimposed peak contact pressure can improve the mechanical properties considerably.

To bridge this huge gap in bonding temperature and to investigate the relation between bonding temperature, contact pressure, and deformation more closely, additional diffusion bonding experiments were performed in the range of $T = 925–975\,°C$. In this range, a strong impact on elongation at fracture was found. Obviously, a further decrease in temperature at a constant contact pressure of $p = 16\,MPa$ is not sufficient for obtaining a sound bond.

From the diffusion bonding results obtained at $T = 850\,°C$ with increasing contact pressure, it was deduced that an increased contact pressure may compensate decreasing elongation at fracture values at low temperatures if deformation during diffusion bonding is increased. To prove this assumption, an additional experiment at $T = 800\,°C$ and a contact pressure of $p = 64\,MPa$ was performed.

In fact, whereas for a bonding temperature of $T = 850\,°C$, the deformation was 8.38% at a contact pressure of $p = 64\,MPa$, at $T = 800\,°C$, it decreased to 2.1%, which is a reasonable value.

3.6. Tensile Test Measurements

The geometry of a tensile test specimen is shown in **Figure 7**.

For fabrication, the height of diffusion bonding specimens after bonding must be sufficient regardless of the deformation. Here, even for a deformation of 20%, a tensile test specimen with larger cross section, e.g., with a diameter of 5 mm, could have been chosen. However, according to our experience, a diameter of 3 mm is sufficient for homogeneous results. Since the goal was to detect tiny deviations in bonding quality originating from imperfect deformation of surface roughness, the smaller geometry was chosen. The tensile test specimens were wire-cut electrical discharge machining (EDM) from diffusion-bonded samples, placing the bonding plane in the middle of the length of the tensile test specimen for arbitrary deformations (**Figure 8**).

Tensile tests were performed for all diffusion bonding experiments. Whereas only one diffusion bonding experiment was done for each set of bonding parameters, five samples for tensile tests were machined from each diffusion bonding sample for statistical reasons. Tensile tests were performed traverse controlled $(dl/dt = 2\,mm\,min^{-1})$ using a universal testing machine from *Instron*, Norwood, USA, type 4505, equipped with a controller unit from *Doli*, Doli Elektronik GmbH, Munich, Germany.

In **Table 3**, yield strength, tensile strength, and elongation-at-fracture values are given for all diffusion bonding experiments performed using samples $d = 40\,mm$, $h = 2 \times 40\,mm$, together with the standard deviation from five specimens each.

In addition, values for delivery condition and a heat treatment at $T = 1100\,°C$ and $t = 4\,h$ are given. Comparing delivery and heat-treated condition, a reduction in yield strength by 25% is found. The tensile strength, however, is reduced by 10% only. This can be attributed to grain growth and reduced dislocation density after the heat treatment. In consequence, the material exhibits more cold work hardening during tensile tests. The travel distance of dislocations to the next obstacle, namely, the
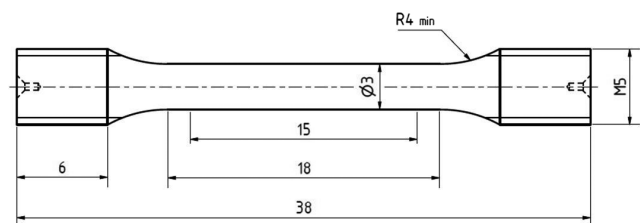

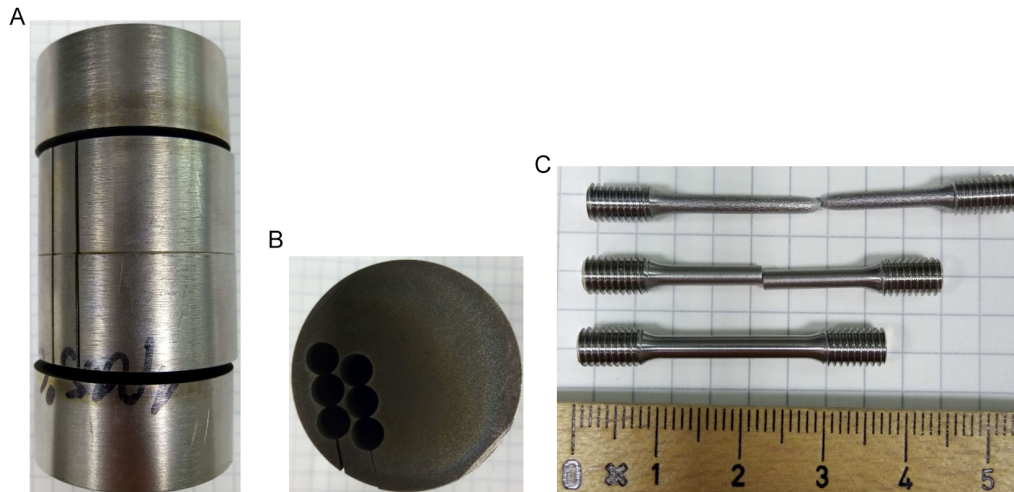**Figure 7.** Dimensions of tensile test specimens.

Figure 8. A,B) Scheme of tensile test specimen manufacturing. C) Bottom: new tensile test specimen. Middle: failure within proportional elongation range at bonding plane. Top: fracture at high strain with necking.

Table 3. Summary of the mechanical strength and elongation-at-fracture values from five tensile test samples each.

T [°C]	p [MPa]	t [h]	Deformation [%]	$R_{p0.2}$ [MPa]	Stand. dev.	R_m [MPa]	Stand. dev.	A_5 [%]	Stand. dev.
Delivery cond.	–	–	–	**304.5**	5.9	**652.7**	2.3	**79.0**	2.0
Heat-treated 1100 °C 4 h^{-1}	–	–	–	**227.0**	7.2	**588.5**	7.2	**95.9**	2.1
800	64	4	2.1	311.0	8.0	545.8	15.3	21.6	2.7
850[a]	16	4	0	/		243.5	16.3	0.8	0
850	16	**16**	0	279.0	1.9	387.4	34.3	6.0	2.7
850	32	4	0.31	279.6	3.9	491.0	15.7	15.7	2.0
850	64	4	8.38	316.0	3.5	638.8	2.4	78.1	4.7
850	$32 + 4 \times 64/1'$	4	0.94	277.2	6.2	595.6	13.9	35.6	4.4
850	$32 + 4 \times 64/5'$	4	1.76	287.6	4.2	612.8	9.2	43.3	4.0
850	$32 + 4 \times 96/1'$	4	4.3	310.8	1.6	632.2	3.7	61.9	5.8
925	16	4	0.71	278.4	6.2	456.8	80.1	13.2	12.5
975	16	4	2.14	249.2	4.6	558.4	25.0	47.9	17.9
995	16	4	3	254.0	2.7	597.0	15.2	84.4	23.7
1015	16	4	4.16	271.4	3.5	633.8	4.5	104.7	1.0
1035	16	4	5.64	261.8	6.0	610.2	3.6	100.5	3.6
1055	16	4	7.81	259.0	13.2	601.4	3.8	105.3	2.2
1075	16	4	10.50	237.0	4.7	592.0	2.3	105.5	8.7
1095	16	4	13.53	250.6	4.3	587.8	2.2	99.6	2.3
1115	16	4	16.00	247.6	1.8	589.0	2.2	105.6	2.0
1135	16	4	19.79	253.8	5.8	593.6	4.6	100.2	3.8

[a]Values of two samples only, no adhesion.

grain boundary, is larger, and the elongation at fracture is increased by 20% related to the delivery condition.

It is noteworthy that the heat-treated sample has a significantly lower value for elongation at fracture than diffusion-bonded samples in the temperature range between 1015 and 1135 °C. Apparently, the deformation during diffusion bonding has a beneficial effect on the materials' microstructure.

From Table 3, four different sections can be clearly distinguished in terms of deformation during diffusion bonding and mechanical properties: 1) diffusion bonding experiments performed at $T = 850$ °C at constant contact pressures. 2) Diffusion bonding experiments performed at $T = 850$ °C at a constant contact pressure of $p = 32$ MPa, superimposed by peak contact pressures. 3) Diffusion bonding experiments using temperature steps of 20 K around the standard bonding

**ADVANCED
SCIENCE NEWS**
www.advancedsciencenews.com

**ADVANCED
ENGINEERING
MATERIALS**
www.aem-journal.com

temperature of $T = 1075\,°C$ in the temperature range of 1015–1135 °C, leading to elongation-at-fracture values of 100–105%. 4) Diffusion bonding experiments between 925 and 995 °C at a constant contact pressure of $p = 16\,MPa$, leading to reduced values for elongation at fracture.

3.6.1. Experiments at $T = 850$ and $800\,°C$, and Constant Contact Pressures

Apparently, a contact pressure of $p = 16\,MPa$ is too low to achieve reasonable mechanical properties at a bonding temperature of $T = 850\,°C$. For $t = 4\,h$, only two samples can be assessed exhibiting less than 0.2% strain. The other three samples separated spontaneously. Even for a dwell time of $t = 16\,h$, the elongation at fracture is only 6%. Values for tensile strength and elongation at fracture possess high standard deviations, underlining scattering within the five samples. There is no visible deformation for both dwell times.

For a contact pressure of $p = 32\,MPa$, a deformation of only 0.31% was obtained. It can be assumed that no good mechanical strength is achievable. However, an identical yield strength as for $p = 16\,MPa$ and $t = 16\,h$ was obtained. The tensile strengths increased by 27% to 491 MPa, and the elongations at fracture increased by the 2.5-fold to 16%. It is noticeable that the tensile strength scatters with a standard deviation of 15.7 MPa, whereas scattering of the elongations at fracture is considerably lower.

For a contact pressure of $p = 64\,MPa$, a deformation of 8.38% was obtained which is too much for most technical applications. For a bonding temperature of $T = 850\,°C$, a reasonable deformation seems to appear in a range between 32 and 64 MPa for the contact pressure, depending on the geometry of the part to be bonded. The yield strength increased by 13% to 316 MPa. However, due to a huge increase in the elongation at fracture from 16% to 78.1%, the tensile strength was raised by 30% from 491 to 639 MPa. The scattering of samples

for all mechanical parameters is reduced in relation to its absolute values.

Comparing the mechanical properties obtained for the diffusion bonding experiment using $T = 850\,°C$, $p = 64\,MPa$, and $t = 4\,h$, the values are fairly identical to those of the delivery state.

To assess if the deformation can be decreased to a technically reasonable value, an additional diffusion bonding experiment with a contact pressure of $p = 64\,MPa$ but a decreased temperature of $T = 800\,°C$ was performed. A deformation of 2.1% was obtained, which is a reasonable value. Whereas the yield strength is comparable to delivery state as well as to 850 °C, 64 MPa, and 4 h, the tensile strength dropped by 15% to 546 MPa, and the elongation at fracture was reduced to 21.6%, which is less than one third.

The results for bonding temperatures of $T = 800$ and 850 °C and constant contact pressures are summarized in **Figure 9**.

3.6.2. Experiments at $T = 850\,°C$, Contact Pressure $p = 32\,MPa$, and Superimposed Peak Contact Pressures

As shown by the diffusion bonding experiments using constant contact pressures of 32 and 64 MPa, it is difficult in this way to achieve a predefined deformation for arbitrary geometries, e.g., for guaranteeing vacuum tightness. However, it shows that the impact of the contact pressure on mechanical strength and especially on elongation at fracture is enormous. Therefore, the idea arose to select the contact pressure for the main dwell time in such a way that only a small time-dependent deformation occurs. A contact pressure of $p = 32\,MPa$ is appropriate since a deformation of only 0.31% occurred within $t = 4\,h$. Increasing the contact area at an atomic scale, however, should be achieved at much higher contact pressures, deforming asperities. Adjusting the dwell time at a high materials flow rate, the overall deformation can be controlled. For this, tests with constant contact pressures offered good approximate values. As peak contact pressures,
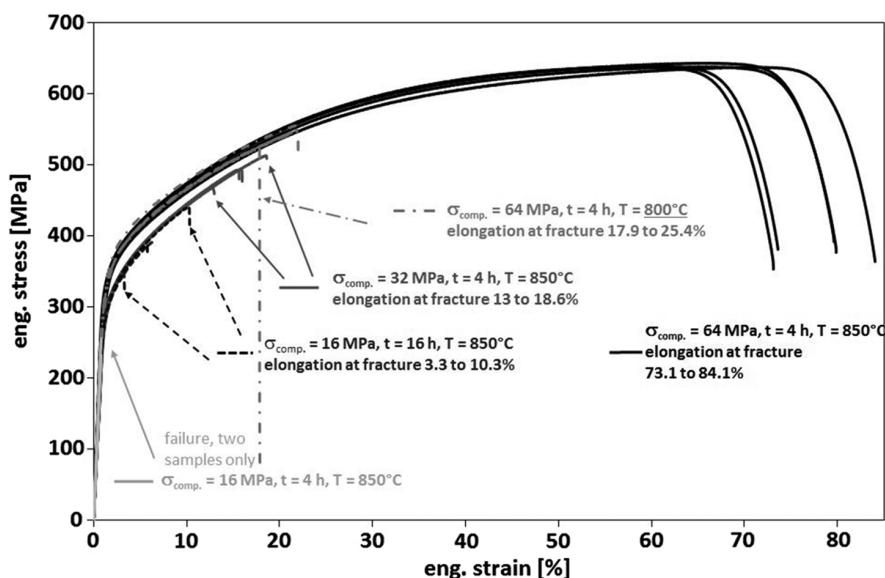

Figure 9. Comparison of the results of tensile tests for low diffusion bonding temperatures of 800 and 850 °C and dwell times of 4 and 16 h, respectively, at constant contact pressures.

**ADVANCED
SCIENCE NEWS**

www.advancedsciencenews.com

**ADVANCED
ENGINEERING
MATERIALS**

www.aem-journal.com

$p = 64$ and 96 MPa were chosen. For $p = 64$ MPa, the dwell time was set to $t = 1$ and 5 min, respectively. A peak contact pressure of $p = 96$ MPa, however, was applied for $t = 1$ min only. From Table 2, it can be seen that the deformation during the diffusion bonding process can be adjusted, and mechanical strength values as well as elongation-at-fracture values are superior compared to constant contact pressure experiments.

Elongation-at-fracture values increase continuously and are sufficient to prevent a catastrophic failure of parts. However, it remains below delivery condition, indicating binding flaws.

The deformation during diffusion bonding can be limited to reasonable values compared to a constant contact pressure of $p = 64$ MPa. **Figure 10** shows all data obtained for diffusion bonding experiments performed at $T = 850\,^\circ$C using superimposed peak contact pressures.

3.6.3. Experiments for Bonding Temperatures Ranging from $T = 1015–1135\,^\circ$C for $t = 4$ h, $p = 16$ MPa

As mentioned earlier, the bonding temperature and contact pressure have an opposite effect on the deformation. Identical deformations can be achieved at a low bonding temperature and high contact pressure as well as high bonding temperature and low contact pressure. The question arises whether there is a sound relation between deformation and mechanical properties.

For this, diffusion bonding experiments with variations in steps of $T = 20$ K around a bonding temperature of $T = 1075\,^\circ$C were performed, covering a range of $T = 1015$ to $1135\,^\circ$C. From Table 3, it can be seen that the deformation increases steadily with temperature. The yield strength and the tensile strength decrease slightly. This can be attributed to grain growth and the Hall–Petch relation.

The values for elongation at fracture, however, are constant within 100–105% for the whole temperature range.

It can be seen that good mechanical properties are obtained for $T = 1015\,^\circ$C and a deformation of 4.16%. The elongation at fracture is 104.7%, whereas for diffusion bonding at $T = 850\,^\circ$C and a short peak contact pressure of $p = 96$ MPa, given a deformation of 4.3%, it is only 61.9%. From this, it can be concluded that a
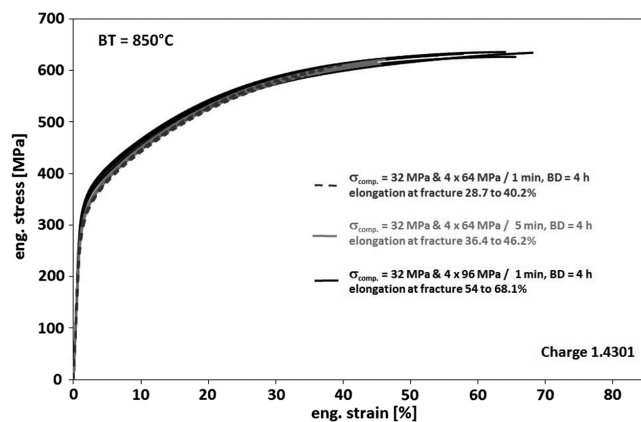

Figure 10. Tensile tests for diffusion bonding at $T = 850\,^\circ$C, $t = 4$ h, and contact pressure of $p = 32$ MPa, and superimposed peak contact pressures.
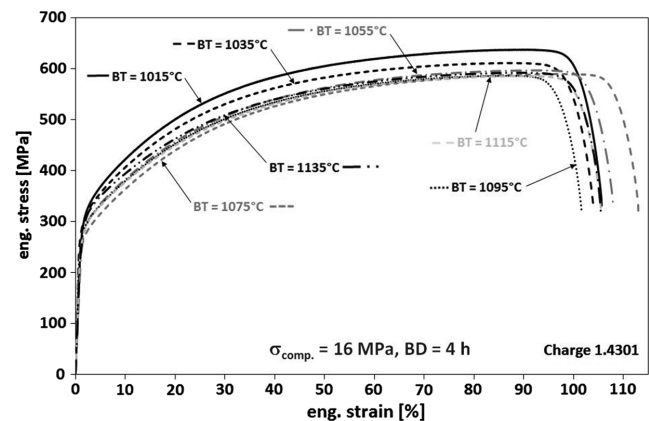

Figure 11. Tensile tests for diffusion bonding between $T = 1015$ to $1135\,^\circ$C, $t = 4$ h (selected samples).

certain deformation is a necessary but not sufficient constraint for identical mechanical parameters.

Figure 11 shows tensile test curves obtained for the temperature range of $T = 1015$ to $1135\,^\circ$C. Since scattering between the five tensile test specimens is small, only one specimen per test condition is shown for clarity.

3.6.4. Experiments for $t = 4$ h, $p = 16$ MPa, and $T = 925$, 975, and $995\,^\circ$C, respectively

To cover the temperature gap between $T = 850$ and $1015\,^\circ$C, as well as the gap for elongations at fracture, additional experiments at intermediate temperatures were performed.

Table 3 shows that the yield strength is maximum for $T = 925\,^\circ$C. This is attributed to the impact of grain growth with temperature. However, the tensile strength shows the opposite trend: it increases for rising temperatures whereas the standard deviation decreases. This is also in accordance with elongation-at-fracture values increasing with temperature. High standard deviations for values of both elongation at fracture and tensile strength indicate imperfect bonding. Apparently, a contact pressure of $p = 16$ MPa is too low to achieve a good and reproducible bond at temperatures of $T = 995\,^\circ$C and below within $t = 4$ h.

The yield strength for $T = 925\,^\circ$C, however, is identically to $T = 850\,^\circ$C, $t = 16$ h at the same contact pressure of $p = 16$ MPa as well as for $p = 32$ MPa and $t = 4$ h. The tensile strength for $T = 925\,^\circ$C, however, is in between these two experiments at $T = 850\,^\circ$C. For $T = 850\,^\circ$C and 32 MPa, the tensile strength is 7% higher (491 MPa) than for $T = 925\,^\circ$C (456.8 MPa) despite the fact that the values for elongation at fracture are nearby and the deformation from the bonding process is lower. However, the tensile strength for $T = 925\,^\circ$C shows a huge scattering (min./max. values for five specimens: 399/593 MPa). Here, further experiments could be performed considering the impact of surface roughness.

For $T = 995\,^\circ$C, the yield strength is 18% lower (254 MPa) than that for the experiment at $T = 850\,^\circ$C, $p = 32$ MPa, and a peak contact pressure of $p = 96$ MPa (310.8 MPa). It is worth mentioning that also the tensile strength is about 5% lower despite the fact that the elongation at fracture was raised from 61.9 to 84.4%. However,
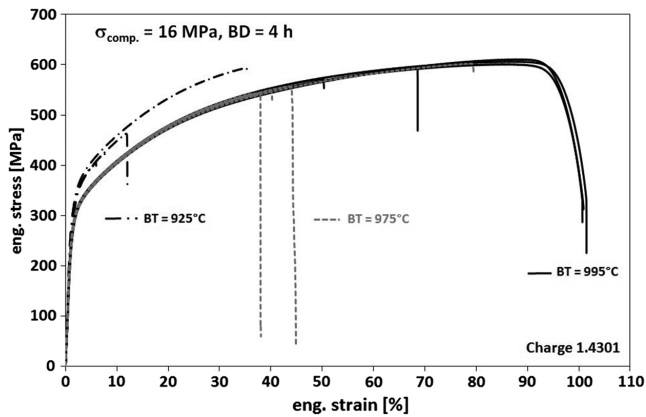
Figure 12. Tensile tests for diffusion bonding for $T = 925$, 975, and 995 °C.

Figure 13. Diffusion bonding experiments according to increasing deformation versus elongations at fracture.

the deformation during the diffusion bonding process for $T = 995$ °C is only two thirds that of the experiment at $T = 850$ °C with a peak contact pressure of $p = 96$ MPa.

Figure 12 shows the curves for bonding experiments performed at $T = 925$, 975, and 995 °C. Due to huge differences in elongation-at-fracture and tensile strength values, different sets of parameters can clearly be distinguished.

3.6.5. Evaluation of the Relationship between Deformation and Elongation at Fracture

From Table 3, three areas of elongations at fracture can be distinguished: First, experiments with nearly no elongation at fracture, namely, for a bonding temperature of $T = 850$ °C in combination with a constant contact pressure of $p = 16$ MPa, leading to zero deformation.

Second, experiments leading to elongations at fracture of about 100%, starting at a minimum bonding temperature of $T = 1015$ °C. The deformation increases continuously from 4.16 to 19.78% with temperature for a constant contact pressure of $p = 16$ MPa.

Third, for varying temperatures and contact pressures as well as contact pressure regimes, the elongations at fracture and deformation vary in a wide range.

These experiments were ordered according to increasing deformations to evaluate if elongations at fracture follow the trend of deformation during diffusion bonding (**Figure 13**). It can be stated that for experiments ranging within $T = 925$–995 °C and a constant contact pressure of $p = 16$ MPa, the deformation and elongations at fracture drop steadily. Obviously, a contact pressure of $p = 16$ MPa is too low to facilitate reasonable elongations at fracture.

In general, the elongations at fracture, even for higher deformations, are lower than the values obtained at a bonding temperature of $T = 1015$ °C and above, which have comparable deformations. The increase in contact pressure cannot compensate for the effect of a decreasing bonding temperature, since the diffusion coefficient is several orders of magnitude lower.
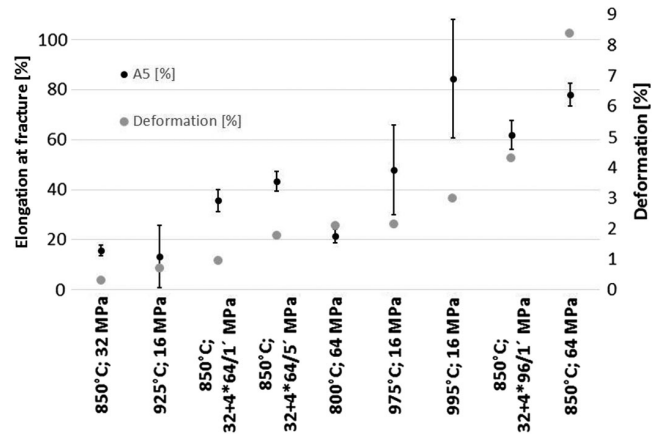
3.7. Evaluation of Fracture Surfaces

The tensile specimens for the temperature range $T = 1015$–1135 °C show a very high elongation at fracture and reduction in area. The remaining cross section shows a ductile fracture with dimples (**Figure 14**).

More interesting is the evaluation of fracture surfaces of diffusion bonding experiments showing strong scattering of elongation-at-fracture values. Minimum and maximum values for elongation-at-fracture data for selected diffusion bonding experiments are given in **Table 4**.

For $T = 850$ °C, $t = 4$ h, and $p = 32$ MPa applying short peak contact pressures of $p = 64$ MPa and a dwell time of $t = 5$ min, machining grooves from turning are visible in the fracture surface despite of the fact that this sample possesses an elongation at fracture of 36.4%. The sample exhibiting the maximum elongation at fracture of 46.2% shows considerably less machining grooves. A reduction in area is not visible (**Figure 15**). Obviously, these elongation-at-fracture values are within the proportional elongation range (Figure 8C, middle). At the same time, the bonding quality is sufficient to deform the full cross-sectional length of the sample.

For $T = 850$ °C, $t = 4$ h, and $p = 32$ MPA applying short peak contact pressures of 96 MPa and a dwell time of 1 min, the overview image of the cross section shows a homogeneous bonding state (**Figure 16**). However, periodic structures are clearly visible. At higher magnification, scratches and remains from turning are visible. For minimum and maximum elongations at fracture of 54% and 68.1%, no obvious reduction in area is visible. An elongation of nearly 70% is obtained in the proportional elongation range.

Looking at samples diffusion-bonded between $T = 925$ to 995 °C at a constant contact pressure of $p = 16$ MPa for $t = 4$ h, a transition of fracture surfaces is found. At $T = 925$ °C, the difference in percentaged bonded cross sections is already obvious at low magnification for minimum and maximum elongations at fracture values of 5.4% and 35%, respectively (**Figure 17**).

For $T = 975$ °C, the difference in bond quality for the samples with minimum and maximum elongations at fracture is clearly visible (**Figure 18**). However, for the sample with the maximum
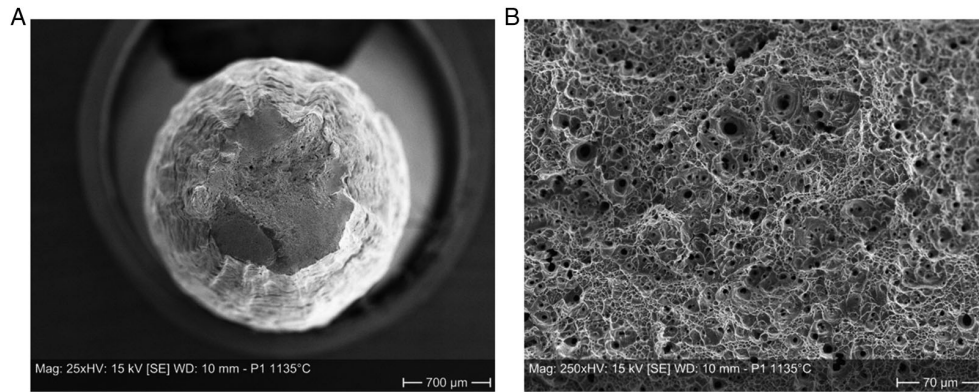
Figure 14. A: Fracture surface of sample No. 1, $T = 1135\,°C$, $t = 4\,h$, and $p = 16\,MPa$. Elongation at fracture: 102.0%. B: Detail of fracture surface.

Table 4. Minimum and maximum values for elongation-at-fracture values from five samples each for selected diffusion bonding experiments.

$T\,[°C]$	$p\,[MPa]$	$t\,[h]$	Deformation [%]	$A_5\,[\%]$	Stand. dev.	A_5 min. [%]	A_5 max. [%]
850	$32 + 4 \times 64/1'$	4	0.94	35.6	4.4	28.7	40.2
850	$32 + 4 \times 64/5'$	4	1.76	43.3	4.0	36.4	46.2
850	$32 + 4 \times 96/1'$	4	4.3	61.9	5.8	54.0	68.1
925	16	4	0.71	13.2	12.5	5.4	35.0
975	16	4	2.14	47.9	17.9	36.8	79.5
995	16	4	3	84.4	23.7	50.4	100.9

elongation at fracture of 35%, an incipient crack seems to have occurred outside the bonding plane. No necking appeared because the bonding plane could not transfer sufficient load.

The greatest differences in bond quality occurred at $T = 995\,°C$. The elongation-at-fracture values are 50% and 100%, respectively, for the worst and best sample. Sample 5 with

50% elongation at fracture shows severe grooves from turning whereas sample 3 bonded at $T = 975\,°C$, having an elongation at fracture of 79.5%, shows nearly no defects. In contrast, sample 3 bonded at $T = 995\,°C$ and 100% elongation at fracture exhibits pronounced necking (**Figure 19**).

Finally, it can be concluded that in the temperature range of $T = 925$ to $995\,°C$, the bond quality scatters extremely within five tensile samples. As long as machining grooves are visible on the bond surfaces, vacuum tightness cannot be expected despite sufficient mechanical properties.

Diffusion bonding experiments performed at $T = 850\,°C$ with superimposed peak contact pressures led to better results.

4. Conclusion and Outlook

Diffusion bonding can be performed successfully in a wide range of temperatures regarding mechanical properties. Even at a bonding temperature of $T = 850\,°C$, it is possible to obtain

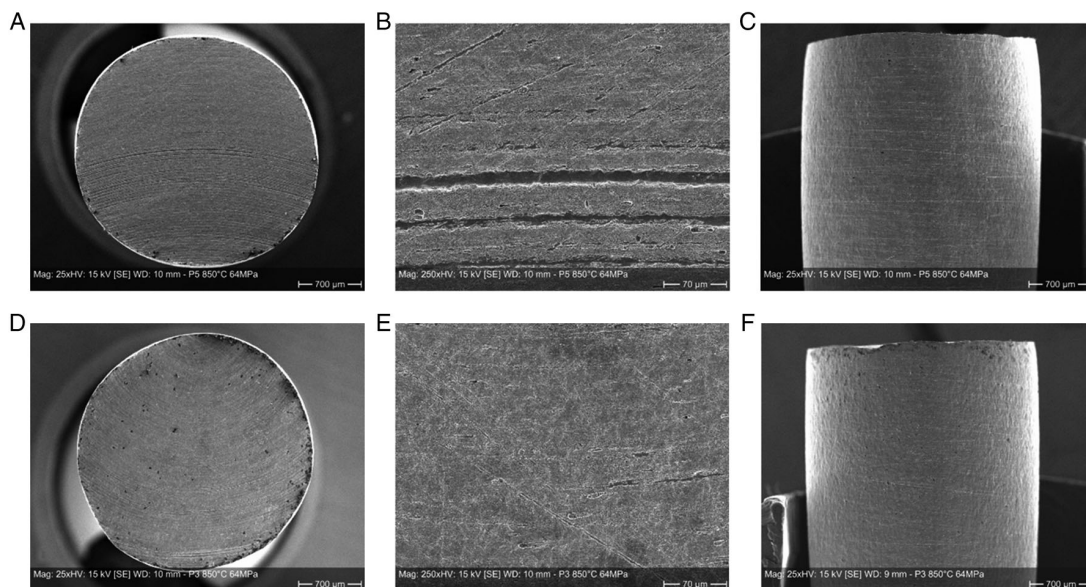**Figure 15.** Fracture surfaces for $T = 850\,°C$, $t = 4\,h$, and $p = 32\,MPa + 4 \times 64\,MPa/5\,min$. A–C) Sample No. 5, $A_5 = 36.6\%$. D–F) Sample No. 3, $A_5 = 46.2\%$.
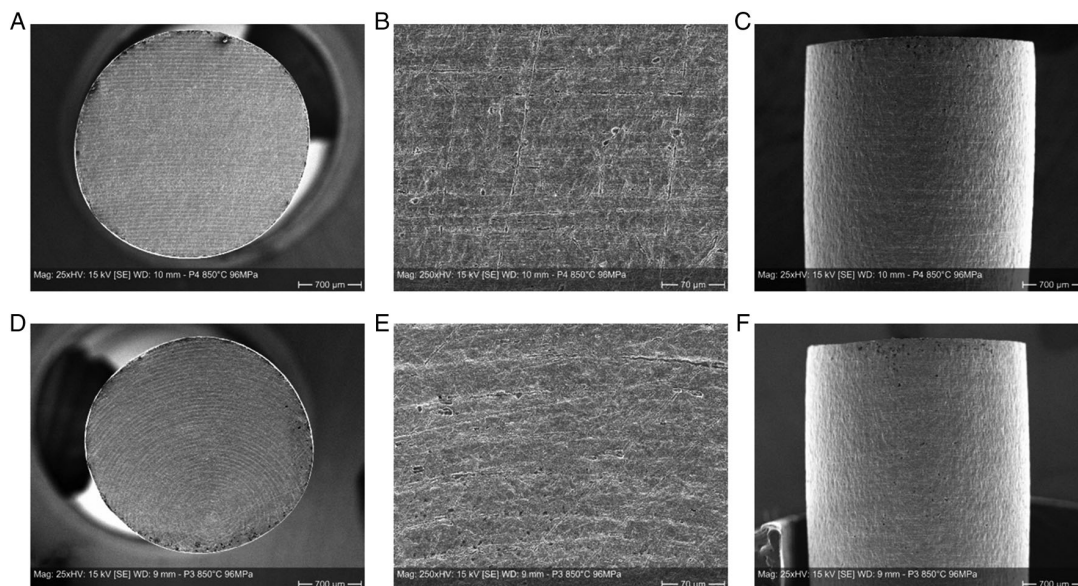
Figure 16. Fracture surfaces for $T = 850\,°C$, $t = 4\,h$, and $p = 32\,MPa + 4 \times 96\,MPa/1\,min$. A–C) Sample No. 4, $A_5 = 54.0\%$. D–F) Sample No. 3, $A_5 = 68.1\%$.

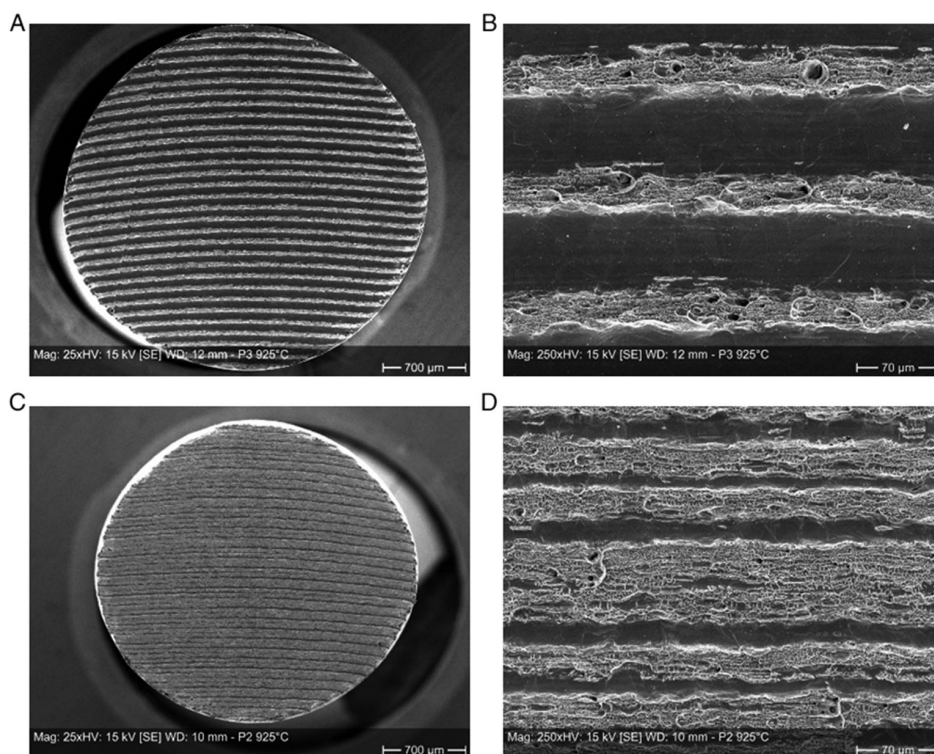**Figure 17.** Fracture surfaces for $T = 925\,°C$, $t = 4\,h$, and $p = 16\,MPa$. A,B) Sample No. 3, $A_5 = 5.4\%$. C,D) Sample No. 2, $A_5 = 35.0\%$.

reasonable elongations at fracture, preventing catastrophic failure of devices.

Diffusion bonding experiments performed in steps of 20 K showed the strong impact of the bonding temperature on deformation. Therefore, it is important to control the temperature precisely.

The experiments proved that it is difficult to define bonding parameters using constant contact pressure to reach a target deformation.

Superimposed short peaks of increased contact pressures lead to reasonable values of elongation at fracture in relation to macroscopic deformation and facilitate leveling of roughness asperities.
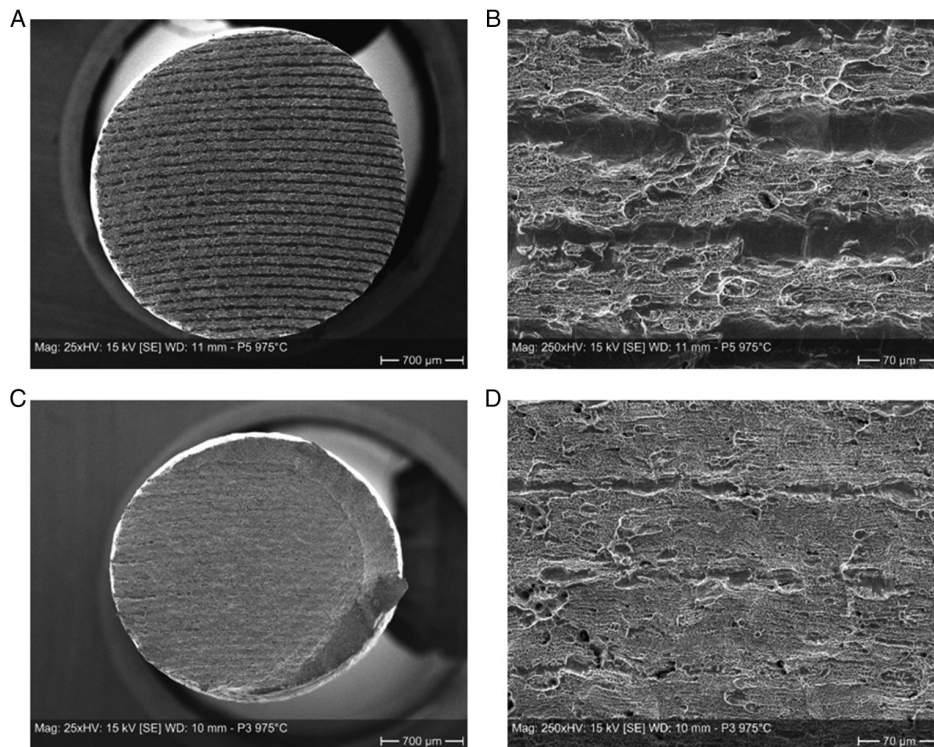
**ADVANCED
SCIENCE NEWS**

www.advancedsciencenews.com

*ADVANCED
ENGINEERING
MATERIALS*

www.aem-journal.com

Figure 18. Fracture surfaces for $T = 975\,°C$, $t = 4\,h$, and $p = 16\,MPa$. A,B) Sample No. 5, $A_5 = 36.8\%$. C,D) Sample No. 3, $A_5 = 79.5\%$.
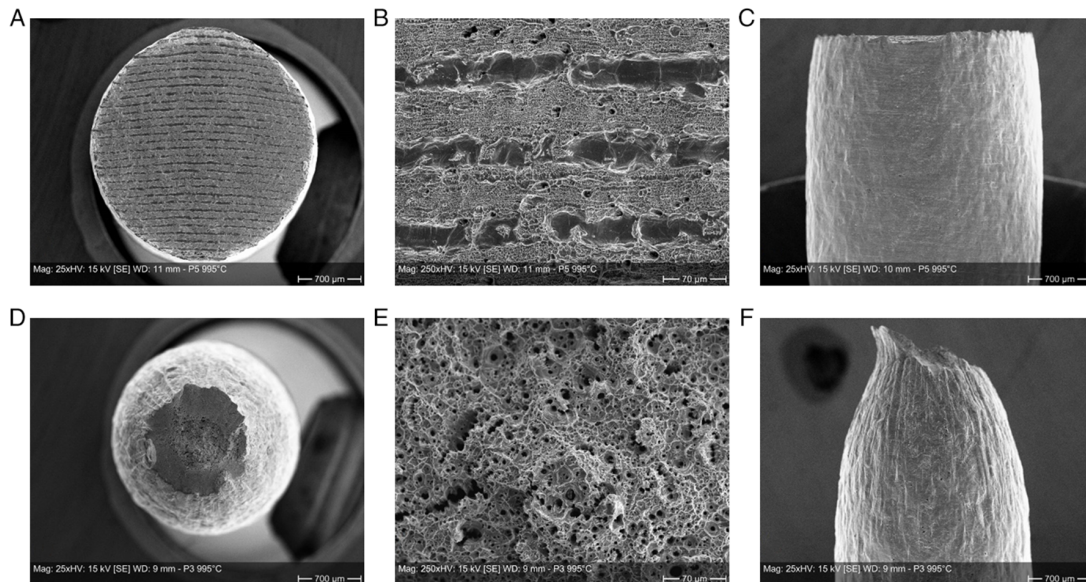

Figure 19. Fracture surfaces for $T = 995\,°C$, $t = 4\,h$, and $p = 16\,MPa$. A–C) Sample No. 5, $A_5 = 50.4\%$. D–F) Sample No. 3, $A_5 = 100.9\%$.

Remaining pores, however, must be filled by volume diffusion. From the experiments, it can be concluded that, at a dwell time of $t = 4\,h$, a bonding temperature of $T = 995\,°C$ does not fulfill this requirement. The elongation at fracture is strongly reduced compared to $T = 1015\,°C$.

Obviously, an increase in contact pressure cannot fully compensate reduced bonding temperature either, even if comparable deformations are obtained. The reason is that the diffusion coefficient in the diffusion bonding temperature range is half for a decrease in 20 K according to the Arrhenius Equation (Equation (1)).[27]

**ADVANCED
SCIENCE NEWS**
www.advancedsciencenews.com

**ADVANCED
ENGINEERING
MATERIALS**
www.aem-journal.com

$$D = D_0 * \exp . \left(\frac{-\Delta U}{RT} \right) \qquad (1)$$

with D diffusion coefficient [$m^2\,s^{-1}$]

D_0 frequency factor (material constant) [$m^2\,s^{-1}$]

U energy of formation of vacancies [$J\,mol^{-1}$]

R gas constant (8.314 $J\,mol^{-1}*K$)

T absolute temperature [K]

It is emphasized that the deformation of the parts to be bonded changes significantly with the geometry. Therefore, these experiments do not necessarily give comparable results in terms of deformation for arbitrary geometries and aspect ratios.

For cylindrical samples of $d = 20$ and 40 mm, respectively, no dependence of the deformation on cross sections was found. Contrary to the findings described in the study by Gietzelt et al.,[9] this is attributed to the high aspect ratio of two and to the fact that the variation in cross sections is low.

Using nonpolymorphic materials, diffusion bonding is accompanied by grain growth. According to the *Hall–Petch* relation, decreasing yield strength and tensile strength have to be expected. Here, a heat treatment at $T = 1100\,°C$, $t = 4\,h$ decreased the yield strength by 25% to 227 MPa and the tensile strength by 10% to 588 MPa, respectively, compared to delivery condition. The elongations at fracture, however, were increased by 21% from 79% to 95.9%. Nevertheless, the mechanical properties meet the specifications of AISI 304 (1.4301) for different dimensions of half stock according to ASTM A276, which have a yield strength of more than 205 MPa, tensile strength of more than 515 MPa, and an elongation at fracture of more than 40%.[28,29]

For diffusion bonding experiments performed in the temperature range of $T = 1015–1135\,°C$, lower bonding temperatures are favorable in terms of yield strength. Starting from $T = 1015\,°C$, the yield strength decreases, and elongation-at-fracture values of at least 100% were obtained.

By decreasing the bonding temperature from $T = 1075–850\,°C$, which is 225 K, and despite decreasing the diffusion coefficient by several orders of magnitude, good mechanical properties and high values for elongation at fracture can be achieved by adjusting the contact pressure and contact pressure regime. The yield strength was slightly increased since the grain growth was lower, even for long dwell times.

Bonding experiments performed between $T = 925$ and 995 °C for a dwell time of $t = 4\,h$ and a constant contact pressure of $p = 16\,MPa$ showed a strong impact of temperature on tensile strength and elongation at fracture. In addition, the standard deviations within the five tensile samples were enormous.

From a practical point of view, the question arises which elongation-at-fracture values are required to reliably exclude unexpected failure of diffusion-bonded components. Face-centered cubic materials in general exhibit very high intrinsic values for elongation at fracture due to the higher number of sliding systems for the dislocation movement. Therefore, for failure safety reasons, values for elongation at fracture for diffusion-bonded components may be defined as for space-centered cubic materials, e.g., mild steels. From this, elongation-at-fracture values of more than 20% appear sufficient. However, these values must be met reliably and must not scatter strongly.

A different point is the application of diffusion-bonded devices, apart from the mechanical properties. Vacuum or water tightness cannot be guaranteed as far as remaining pores are present at the bonding plane. As revealed by the experiments, there is no strong correlation between deformation during diffusion bonding and a bonding plane free of pores.

For austenitic stainless steels containing 18% of chromium and 10% of nickel, a bonding temperature of $T = 1015\,°C$ is sufficient for diffusion bonding.

A quality criterion for a perfect diffusion bond is always grain growth across the bonding planes. In a previous publication, it was shown that the thickness of passivation layers has a huge impact on diffusion bonding results.[10] Due to the different crystallographic or amorphous structures of passivation layers, it hinders the diffusion of atoms across the bonding plane extremely. In addition, the composition of an alloy and its content of metals forming the passivation layer is important in terms of diffusion bonding. Bonding parameters, e.g., suited for an austenitic stainless steel containing 18% of chromium and 10% of nickel cannot be successfully adopted for a nickel-base alloy, e.g., Hastelloy C-22 (2.4602). Not only is the composition of the passivation layer different but also the deformation behavior is different.

As investigated in detail,[30] also the grain size and composition of an alloy have an impact on the deformation behavior at high temperatures.

To overcome these obstacles, the concept of short-term increased contact pressure might be helpful to penetrate passivation layers by surface asperities as well as to limit overall deformation.

Further investigations will be performed regarding the impact of the dwell time of peak contact pressures and its absolute level on the plastic deformation and the bonding result. Since the contact area on the atomic level is increased with time, increasing peak contact pressures or dwell times are also feasible as shown in Figure 5 (for $y_1 < y_2 < y_3 < y_4$ and/or $z_1 < z_2 < z_3 < z_4$, respectively). The dwell time in between peak contact pressures, however, must be sufficient to fill remaining pores by volume diffusion.

Conflict of Interest

The authors declare no conflict of interest.

Data Availability Statement

Research data are not shared.

[1] S. Jahn, *Ph.D. Thesis*, TU Ilmenau, **2007**.

[2] *Einführung In Die Werkstofftechnik*, 6th Ed., (Ed: W. Schatt), Verlag für Grundstoffindustrie, Leipzig **1972**, p. 257.

[3] C. Zhang, H. Li, M. Q. Li, *Appl. Surf. Sci.* **2016**, *371*, 407.

[4] G. Thirunavukarasu, S. Kundu, T. Laha, D. Roy, S. Chatterje, *Metall. Res. Technol.* **2018**, *115*, 115.

[5] G. Thirunavukarasu, S. Kundu, V. V. Patel, A. Alankar, *Diff. Found.* **2020**, *27*, 3.

[6] D. Mo, T. Song, Y. Fang, X. Jiang, C. Q. Luo, M. D. Simpson, Z. Luo, *Adv. Mater. Sci. Eng.*, **2018**, 1.

[7] V. Srikanth, A. Laik, G. K. Dey, *Mater. Des. 126*, **2017**, 141.

[8] I. Sah, D. Kim, H. J. Lee, C. Jang, *Mater. Des.* **2013**, *47*, 581.

[9] T. Gietzelt, V. Toth, A. Huell, R. Dittmeyer, *Adv. Eng. Mater.* **2017**, *19*.

[10] T. Gietzelt, V. Toth, T. Weingärtner, *Mater. Werkstofftech.* **2019**, *50*, 1.

[11] H. Kellerer, *J. Mater. Technol.* **1972**, *3*, 250.

[12] E. O. Hall, *Proc. Phys. Soc. B* **1951**, *64*, 747.

[13] R. W. Armstrong, *Acta Mech.*, **2014**, *225*, 1013.

[14] T. Harumoto, Y. Yamashita, O. Ohashi, T. Ishiguro, *Mater. Trans.*, **2014**, *55* 633.

[15] S. Noh, A. Kimura, T. K. Kim, *Fusion Eng. Des.* **2014**, *89*, 1746.

[16] M. Katoh, N. Sato, T. Shiratori, Y. Suzuki, *ISIJ Int.* **2017**, *57*, 883.

[17] S.-X. Li. F.-Z. Xuan, S.-T. Tu, S.-R. Yu, *Mat. Sci. Eng. A* **2008**, *491*, 488.

[18] Material Data Sheet No. 4121 of 2.4602, version November 2020 by VDM metals, https://www.vdm-metals.com/fileadmin/user_upload/ Downloads/Data_Sheets/Datenblatt_VDM_Alloy_22.pdf, (accessed: October, 2021)

[19] R. Kirchheiner, M. Koehler, U. Heubner, *Werkst. Korros.* **1992**, *43*, 388.

[20] L. B. Mateus, G. Rosinski, P. da Costa Goncalves, M. V. V. Mortean, R. H. Goncalves e Silva, A. S. Monteiro, M. H. B. Mantelli, *24th ABCM Int. Congress of Mech. Eng*, December 2017, Curitiba, PR, Brazil.

[21] X. Ren, S. Li, Z. Xiong, *J. Manuf. Processes* **2018**, *34*, 215.

[22] I. Jauhari, H. Ogiyama, H. Tsukuda, *Mater. Sci. Res. Int.* **2003**, *9* 154.

[23] J. Moravec, I. Novakova, *Key Eng. Mater.* **2017**, *737*, 101.

[24] M. Elßner, S. Weis, T. Grund, G. Wagner, S. Habisch, P. Mayr, *IOP Conference Series: Materials Science and Engineering, 18th Chemnitz Seminar on Materials Engineering - 18. Werkstofftechnisches Kolloquium 10–11 March*, Chemnitz, Germany, Vol. *118*, **2016**, pp. 1–11, https://doi.org/10.1088/1757-899X/118/1/012037, .

[25] J. Han, G. M. Sheng, X. L. Zhou, J. X. Sun, *ISIJ Int.* **2009**, *49*, 86.

[26] G. Sharma, D. K. Dwivedi, *Int. J. Adv. Manuf. Technol.* **2018**, *95*, 4293.

[27] P. I. Williams, R. G. Faulkner, *J. Mater. Sci.* **1987**, *22*, 3537.

[28] Material data sheet for 1.4301 by DEW-Stahl, https://www.dew-stahl.com/fileadmin/files/dew-stahl.com/documents/Publikationen/ Werkstoffdatenblaetter/RSH/1.4301_de.pdf, (Accessed: October 2021).

[29] Material data base WIAM Metallinfo, IMA Materialforschung und Anwendungstechnik GmbH, Dresden, Germany.

[30] H. J. Frost, M. F. Ashby, Deformation-Mechanism Maps, The Plasticity and Creep of Metals and Ceramics", chapter 7, https:// engineering.dartmouth.edu/defmech/, (Accessed: February, 2021).